Radio Pulsars as a Laboratory for Strong-Field Gravity Tests

12

Lijing Shao

Abstract

General relativity offers a classical description to gravitation and spacetime, and is a cornerstone for modern physics. It has passed a number of empirical tests with flying colours, mostly in the weak-gravity regimes, but nowadays also in the strong-gravity regimes. Radio pulsars provide one of the earliest extrasolar laboratories for gravity tests. They, in possession of strongly self-gravitating bodies, i.e. neutron stars, are playing a unique role in the studies of strong-field gravity. Radio timing of binary pulsars enables very precise measurements of system parameters, and the pulsar timing technology is extremely sensitive to various types of changes in the orbital dynamics. If an alternative gravity theory causes modifications to binary orbital evolution with respect to general relativity, the theory prediction can be confronted with timing results. In this chapter, we review the basic concepts in using radio pulsars for strong-field gravity tests, with the aid of some recent examples in this regard, including tests of gravitational dipolar radiation, massive gravity theories, and the strong equivalence principle. With more sensitive radio telescopes coming online, pulsars are to provide even more dedicated tests of strong gravity in the near future.

L. Shao (✉)
Kavli Institute for Astronomy and Astrophysics, Peking University, Beijing, China

National Astronomical Observatories, Chinese Academy of Sciences, Beijing, China
e-mail: lshao@pku.edu.cn

C. Pfeifer, C. Lämmerzahl (eds.), *Modified and Quantum Gravity*, Lecture Notes in Physics 1017, https://doi.org/10.1007/978-3-031-31520-6_12

12.1 Introduction

Pulsars are rotating magnetized neutron stars. On the one hand, due to their large moment of inertia ($I \sim 10^{38}\,\mathrm{kg\,m^2}$) and usually small external torque, their rotation is extremely stable. If a pulsar sweeps a radiating beam in the direction of the Earth, a radio pulse could be recorded using large-area telescopes for each rotation. As fundamentally known in physics, such a periodic signal can be viewed as a *clock*. Therefore, pulsars are famously recognized as astrophysical clocks in astronomy. Even better, thanks to a sophisticated technique called pulsar timing [58], pulsar astronomers can *accurately* record a number of periodic pulse signals. These pulses' times of arrival are compared with atomic clocks at the telescope sites. Some of these observations can be carried out and last for decades. From a large number of times of arrival of these pulse signals, the physical properties of pulsar systems are inferred to a great precision [39]. For example, a recent study with 16 years of timing data of the Double Pulsar,[1] PSR J0737−3039A/B, gives the rotational frequency of pulsar A in the binary system [37],

$$\nu = 44.054068641962 81(17)\,\mathrm{Hz}\,. \tag{12.1}$$

It has sixteen significant digits, and the numbers in the parenthesis give the uncertainty of the last-two digits. Such a precision rivals the precision of atomic clocks on the Earth [30], and also it possibly calls for an extension of the usual use of floating numbers in computer numerics for future precision pulsar timing experiments. Pulsars are truly *precision clocks*.

? Exercise

12.1. During the 16 years of observation, how many cycles have PSR J0737−3039A rotated?

On the other hand, neutron stars are the densest objects known that are made of standard-model materials. For such a compact object, gravity plays a vital role in shaping its internal structure and affecting its external dynamics. As explicitly demonstrated by Damour and Esposito-Farèse [16], if gravity is described by an alternative theory to the general relativity—in their case, a class of scalar-tensor gravity theories—nonperturbative phase-transition-like behaviours might happen for neutron stars, resulting in large deviations from general relativity in the strong field of neutron stars [17, 25, 46]. These large deviations will manifest in the timing

[1] Currently, PSR J0737−3039A/B is the only discovered double neutron star system whose two neutron stars were both detected as pulsars [14, 41, 49], known as Pulsar A and Pulsar B.

data of pulsars in some way (cf. Sect. 12.2), and they could provide smoking-gun signals for gravity theories regarding the strong-field properties. Combining the strong-field nature of neutron stars and the precision measurements of times of arrival, radio pulsars are truly ideal to test alternative theories of gravity [51,63,64], augmenting what have been done in the weak field of the Solar System [65], and complementing what are recently being performed with gravitational waves [3–5] and black hole shadows [6–8,50].

Currently, more than three thousands of radio pulsars are discovered[2] [43]. The most useful subset of pulsars in testing alternative gravity theories are millisecond pulsars in *clean* binaries.[3] Their times of arrival at telescopes are imprinted with information from the following sources:

1. the Solar system dynamics which affect the motion of radio telescopes;
2. the binary dynamics which are resulted from the mutual gravitational interaction between the two binary components; and
3. the interstellar medium which affects the propagation of radio waves in a frequency-dependent way, in terms of dispersion, scattering, and so on.

A formalism, which includes the above effects and connects the proper time of the pulse signals in the pulsar frame to the observed coordinate time at the telescopes, is called a *pulsar timing model*. One of the widely used timing models for binary pulsars is the Damour-Deruelle timing model [15]. It is a phenomenological model that applies to a large set of alternative gravity theories which are possibly being the underlying theory for the binary's orbital motion.

In the Damour-Deruelle timing model, a handful of parameterized post-Keplerian (PPK) parameters are introduced for generic Lorentz-invariant extensions of gravity theories [19]. The values of PPK parameters differ in different gravity theories. Therefore, measurements of these PPK parameters can be converted into constraints on parameters in the alternative gravity theories. The most frequently used PPK parameters include $\dot{\omega}$, $\dot{P}_{\rm b}$, γ, r, and s. The PPK parameter $\dot{\omega}$ describes the periastron advance of the binary orbit, the PPK parameter $\dot{P}_{\rm b}$ describes the orbital period decay caused by the radiation of gravitational waves, the PPK parameter γ describes combined effects from the Doppler time delay and gravitational time delay, and the PPK parameters (r, s) describe the Shapiro time delay imprinted by the spacetime curvature of the companion star. The values of these five PPK parameters in the

[2] https://www.atnf.csiro.au/people/pulsar/psrcat/.

[3] In one case, a pulsar in a triple system, PSR J0337+1715, provides the best limit on the strong equivalence principle [9,47,59].

general relativity are given in Damour and Deruelle [15] and Lorimer and Kramer [39],

$$\dot{\omega} = 3\left(\frac{P_{\rm b}}{2\pi}\right)^{-5/3}(T_\odot M)^{2/3}\left(1-e^2\right)^{-1}, \tag{12.2}$$

$$\dot{P}_{\rm b} = -\frac{192\pi}{5}\left(\frac{P_{\rm b}}{2\pi}\right)^{-5/3}\left(1+\frac{73}{24}e^2+\frac{37}{96}e^4\right)\left(1-e^2\right)^{-7/2}T_\odot^{5/3}m_{\rm A}m_{\rm B}M^{-1/3}, \tag{12.3}$$

$$\gamma = e\left(\frac{P_{\rm b}}{2\pi}\right)^{1/3}T_\odot^{2/3}M^{-4/3}m_{\rm B}(m_{\rm A}+2m_{\rm B}), \tag{12.4}$$

$$r = T_\odot m_{\rm B}, \tag{12.5}$$

$$s = x\left(\frac{P_{\rm b}}{2\pi}\right)^{-2/3}T_\odot^{-1/3}M^{2/3}m_{\rm B}^{-1}, \tag{12.6}$$

where $P_{\rm b}$ and e are respectively the orbital period and orbital eccentricity, $m_{\rm A}$ and $m_{\rm B}$ are the masses of the pulsar and its companion in unit of the Solar mass ($M_\odot$), the total mass $M \equiv m_{\rm A}+m_{\rm B}$, and $T_\odot \equiv GM_\odot/c^3 = 4.925490947\,\mu$s. Equations (12.2)–(12.6) take different forms in alternative gravity theories, often with dependence on the extra charges of the binary components in the theory, e.g., these PPK parameters depend on scalar charges of the pulsar and its companion in the scalar-tensor theory [17]. In pulsar-timing observation, each PPK parameter is *independently* measured. Eventually, for a gravity theory to pass the tests from pulsar timing, it should give consistent predictions to *all* the measured values of PPK parameters with a *unique* set of physical parameters of the binary system. These consistency checks are often illustrated in the mass-mass diagram. For an example, in Fig. 12.1 the measurements of three PPK parameters, $\dot{\omega}$, γ, and $\dot{P}_{\rm b}$, from the Hulse-Taylor pulsar PSR B1913+16, give consistent component masses when the general relativistic Eqs. (12.2)–(12.4) are used [61]. Therefore, general relativity passes the tests posed by the Hulse-Taylor pulsar [61].

? Exercise

12.2. For the Hulse-Taylor pulsar PSR B1913+16, the following parameters are measured directly via pulsar timing: $P_{\rm b} = 0.322997448918(3)\,$d, $e = 0.6171340(4)$, $\dot{\omega} = 4.226585(4)\,$deg yr^{-1}, and $\gamma = 0.004307(4)\,$s [61]. Assuming general relativity, please derive the two component masses for this binary system.

In this following, we will give a few more concrete and recent examples where binary pulsars play a key role in limiting alternative gravity theories, including the gravitational dipolar radiation in the scalar-tensor gravity (Sect. 12.2), two

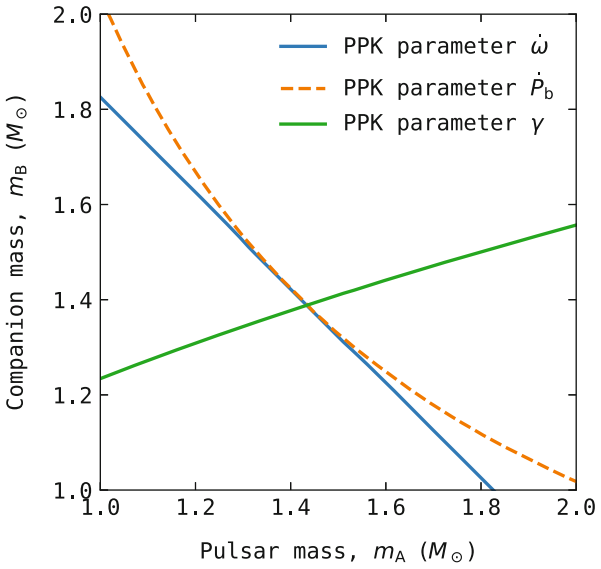

Fig. 12.1 Consistency of general relativity in describing three measured PPK parameters ($\dot{\omega}$, γ, and $\dot{P}_b$) from PSR B1913+16 in the mass-mass diagram [61]

classes of massive gravity theories (Sect. 12.3), and the strong equivalence principle (Sect. 12.4). These examples are by no means complete, and certainly reflect the somehow biased topics that the author is interested in. A short perspective discussion is given in Sect. 12.5. For more extensive reviews on using radio pulsars for gravity tests, readers are referred to Refs. [35, 42, 51, 57, 63, 64].

12.2 Strong-Field Effects and Gravitational Dipolar Radiation

Scalar-tensor gravity theories represent a well posed, healthy extension of Einstein's general relativity by including a nonminimally coupled scalar field in the Lagrangian of gravity [10, 13, 65]; see also Sects. 4.4.4 and 7.4.1 for the discussion of gravity theories involving additional scalar fields as mediator of the gravitational interaction. Shortly after the first discovery of the Hulse-Taylor binary pulsar, Eardley [24] pointed out that a gravitational dipolar radiation could be used as a discriminant for such a class of gravity theories. An extra dipolar radiation term can be tested with the PPK parameter $\dot{P}_b$. Investigation along this line was boosted by the theoretical discovery that in a slightly extended version of the original scalar-tensor gravity, nonperturbative effects develop for certain neutron stars [16, 17]. The so-called *spontaneous scalarization* (see also Sect. 7.4.1 for more details) introduces a much enhanced gravitational dipolar radiation for a scalarized neutron star in a binary. The dipolar radiation in principle can even dominate over the quadrupolar radiation predicted by the general relativity in binary pulsar observations [cf. Eq. (12.3)], but still keeping all weak-field gravity tests satisfied. This enters the regime of *strong-field* gravity tests, where weak-field tests have a rather limited power.

A general class of scalar-tensor gravity theories have the following action in the Einstein frame,

$$S = \frac{c^4}{16\pi G_*} \int \frac{\mathrm{d}^4 x}{c} \sqrt{-g_*} \left[R_* - 2 g_*^{\mu\nu} \partial_\mu \varphi \partial_\nu \varphi - V(\varphi) \right] + S_\mathrm{m} \left[\psi_\mathrm{m}; A^2(\varphi) g^*_{\mu\nu} \right] , \tag{12.7}$$

where $g_*^{\mu\nu}$ and R_* are the metric tensor and Ricci scalar respectively, ψ_m collectively denotes standard-model matter fields, φ is an extra scalar field, and quantities with stars are in the Einstein frame. The novel aspect lies in the fact that it is a conformal metric $A^2(\varphi) g^*_{\mu\nu}$ instead of $g^*_{\mu\nu}$ itself that couples to matter fields. Such a *nonminimal* coupling is important for the discussions below.

The class of scalar-tensor gravity theories carefully examined by Damour and Esposito-Farèse [16, 17] has

$$V(\varphi) = 0 , \tag{12.8}$$

$$A(\varphi) = \exp\left(\beta_0 \varphi^2 / 2 \right) , \tag{12.9}$$

$$\alpha_0 = \beta_0 \varphi_0 , \tag{12.10}$$

where φ_0 is the asymptotic value of φ at infinity, and α_0 and β_0 are two theory parameters. This is the class of scalar-tensor theories, sometimes denoted as $T_1(\alpha_0, \beta_0)$ and called the *Damour-Esposito-Farèse theory*, that are most widely confronted with pulsar observations [28, 53, 63, 71].

? Exercise

12.3. Derive field equations for the Damour-Esposito-Farèse theory.

? Exercise

12.4. Based on the field equations, derive the modified Tolman-Oppenheimer-Volkoff equations for the Damour-Esposito-Farèse theory, for a spherically symmetric neutron star.

By integrating the modified Tolman-Oppenheimer-Volkoff equations derived from theory (12.7), one gets a boost in a neutron star's scalar charge when its mass reaches a critical point. This phenomenon is understood from the viewpoint of Landau's phase transition theory when a tachyonic instability kicks in and

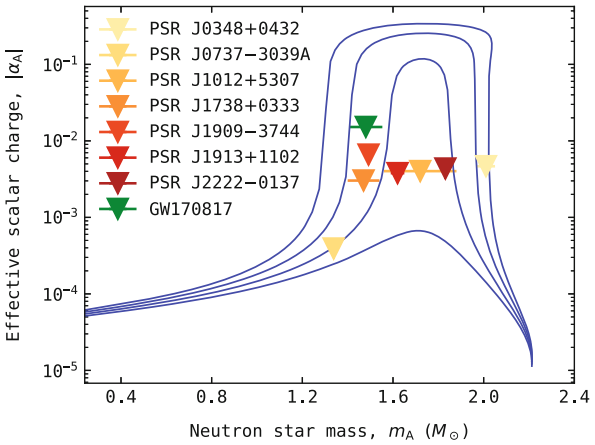

Fig. 12.2 Blue curves show the effective scalar charge in the Damour-Esposito-Farèse scalar-tensor gravity theory with $|\alpha_0| = 10^{-5}$ and, from top to bottom, $\beta_0 = -4.8, -4.6, -4.4, -4.2$. The AP4 equation of state is assumed in the calculation. Triangles show the observational bounds from binary pulsars [53, 71] and gravitational waves [1, 2] at the 90% confidence level. The mass uncertainty for these neutron stars is indicated at the 68% confidence level

a new branch of neutron star solutions with scalar charges are energetically favored [25, 34, 46]. We define the *effective scalar charge* of a neutron star [16],

$$\alpha_A \equiv \frac{\partial \ln m_A}{\partial \varphi_0}, \tag{12.11}$$

which is a representative quantity characterizing the strength of deviation from general relativity. In Fig. 12.2, example curves for the effective scalar charge as a function of neutron star mass are given in blue lines from top to bottom for $\beta_0 = -4.8, -4.6, -4.4, -4.2$, assuming the AP4 equation of state and $|\alpha_0| = 10^{-5}$. As we can easily seen, indeed that for certain mass range of neutron stars, $|\alpha_A|$ can be very large while keeping its value very small in weak-gravity fields.

The emission of gravitational dipolar radiation in a binary pulsar is proportional to the difference in the effective scalar couplings of the two binary components A and B, and to the leading order, it contributes to an additional decay rate of orbital period via [17],

$$\dot{P}_b^{\rm dipole} = -\frac{2\pi G_*}{c^3}\left(1+\frac{e^2}{2}\right)\left(1-e^2\right)^{-5/2}\left(\frac{2\pi}{P_b}\right)\frac{m_A m_B}{M}(\alpha_A-\alpha_B)^2 . \tag{12.12}$$

While neutron stars have significant scalar charges, white dwarfs, being weak-field objects, are hardly different from their counterparts in general relativity with a vanishingly small scalar charge $\alpha_B \simeq \alpha_0 \to 0$, where α_0 is well constrained by Solar System weak-field tests [65]. Therefore, neutron-star white-dwarf binaries turn out

to be the most sensitive probe in this regard [28, 53]. Recently, a new study [71] shows explicitly that neutron-star neutron-star binaries with a significant difference in the masses of binary components are also excellent laboratories. Therefore, to test the gravitational dipolar radiation in scalar-tensor gravity, asymmetric binary pulsars are needed[4] [63].

? Exercise

12.5. When the dipolar-radiation-induced orbital decay is comparable to the quadrupolar-radiation-induced orbital decay for the Hulse-Taylor pulsar? Derive the critical value for the effective scalar charge.

Some illustration for a specific equation of state, `AP4`, is given in Fig. 12.2, along with constraints on the gravitational dipolar radiation from seven binary pulsars [71]: five neutron-star white-dwarf binaries (PSRs J0348+0432, J1012+5307, J1738+0333, J1909−3744, and J2222−0137) and two asymmetric neutron-star neutron-star binaries (PSRs J0737−3039A and J1913+1102). For comparison, we also show a constraint from the first binary neutron star merger observed via gravitational waves [2]. In principle, the uncertainty in the superanuclear neutron-star matter is entangled with strong-field gravity tests [48]. Nevertheless, nowadays we have enough well-measured binary pulsar systems to populate the whole mass range for neutron stars, and a combined study [53, 71] has verified that for each reasonable equation of state, the possibility for spontaneous scalarization in the Damour-Esposito-Farèse scalar-tensor gravity theory is very low. Following the method developed by Shao et al. [53], a dedicated Bayesian parameter-estimation study combining the above-mentioned seven pulsar systems has basically closed the possibility of developing spontaneous scalarization for an effective scalar coupling larger than 10^{-2} for the theory given by Eqs. (12.7)–(12.10), no matter of the underlying yet-uncertain equation of state for supranuclear neutron-star matters.

It is worth to mention that, when performing Markov-chain Monte Carlo Bayesian parameter estimation, the integration of the modified Tolman-Oppenheimer-Volkoff equations needs to be carried out by more than millions of times on the fly thus computationally expensive. Recently, reduced-order surrogate models, which extract dominating features to represent accurate enough integration results, were bulit to aid the speedup of the calculation [29, 70]. The codes of these reduced-order surrogate models are publicly available at https://github.com/BenjaminDbb/pySTGROM and https://github.com/mh-guo/pySTGROMX for community use.

[4] Unfortunately, we have not detected yet suitable neutron-star black-hole binaries for this test, which are also potentially very good testbeds [38].

Although the original Damour-Esposito-Farèse scalar-tensor gravity theory is disfavored by binary pulsar timing results, in further extended, generic scalar-tensor gravity theories, neutron stars can still be scalarized. This is particularly true for a massive scalar-tensor theory with $V(\varphi) \sim m^2\varphi^2$ when the Compton wavelength of the scalar field is smaller than the orbital separation of the binary [45, 66, 69]. Basically the modification with respect to the general relativity in the orbital dynamics is suppressed exponentially in a Yukawa fashion. Fortuitously, without giving much details, such kind of massive scalar-tensor theories can be efficiently probed via the tidal deformability measurement in gravitational waves [1, 31, 32]. In this sense, a combination of pulsar timing data and gravitational wave data is called for to probe a larger parameter space for scalar-tensor gravity theories [53].

In the past few years, other variants of scalar-tensor gravity theories triggered great enthusiasm. Some of them not only give scalarized neutron stars, but also scalarized black holes, in contrast to the *no-hair theorem*. A particularly interesting class of such theory includes a topological Gauss-Bonnet term,

$$\mathcal{G} = R_{\alpha\beta\gamma\delta}R^{\alpha\beta\gamma\delta} - 4R_{\alpha\beta}R^{\alpha\beta} + R^2\,, \tag{12.13}$$

coupling to the scalar field [23, 56, 67]. In Eq. (12.13), $R_{\alpha\beta\gamma\delta}$ and $R_{\alpha\beta}$ are the Riemann tensor and Ricci tensor respectively. Preliminary constraints on the scalar-Gauss-Bonnet gravity from binary pulsars are presented by Danchev et al. [20]. This is a new field where observations of compact objects including neutron stars and black holes are crucial to reveal the strong-field information of gravitation.

12.3 Radiative Effects in Massive Gravity Theories

Radiative tests from binary pulsars are powerful, as the related PPK parameter, $\dot{P}_b$, can be very well measured from a long-term timing project on suitable pulsars [19]. This parameter improves with observational time span $T_{\rm obs}$ quite fast, as $T_{\rm obs}^{-5/2}$. The orbital decay rate $\dot{P}_b$ is not only useful for constraining the dipolar gravitational wave emission, but also in other radiative aspects of gravitation, for example, in constraining the extra radiation caused by a certain model of the breaking down of the Lorentz symmetry [68],[5] or a nonzero mass of gravitons [21, 26, 44, 55]. Here we give a brief introduction to the latter.

In general relativity, the hypothetical quantum particle for gravity, graviton, is a massless spin-2 particle. However, massive gravity theories are found to provide interesting phenomena related to the evolution of the Universe, e.g. the accelerated expansion and dark energy [21]. Therefore, probing the upper bounds of the graviton mass is fundamentally important to field theories and cosmology studies, and it is one of the central topics in gravitational physics.

[5] Recall that there are numerous different models of Lorentz invariance violation or doubly special relativity, see Chaps. 1 or 2.

One of the early study of using binary pulsars to test the graviton mass was performed by Finn and Sutton in 2002 [26]. They investigated a linearized gravity with a massive graviton with the action,

$$S = \frac{1}{64\pi}\int \mathrm{d}^4x\Big[\partial_\lambda h_{\mu\nu}\partial^\lambda h^{\mu\nu} - 2\partial^\nu h_{\mu\nu}\partial_\lambda h^{\mu\lambda} + 2\partial^\nu h_{\mu\nu}\partial^\mu h - \partial^\mu h\partial_\mu h - 32\pi h_{\mu\nu}T^{\mu\nu} + m_{\rm g}^2\left(h_{\mu\nu}h^{\mu\nu} - \frac{1}{2}h^2\right)\Big], \tag{12.14}$$

where the last term gives a unique graviton mass under certain conditions[6] [26] while the others are just linearized expansions from the Einstein-Hilbert action with $h_{\mu\nu} \equiv g_{\mu\nu} - \eta_{\mu\nu}$ and $h \equiv h^\mu{}_\mu$. It was shown that extra gravitational wave radiation exists in theory (12.14), which results in a fractional change in the orbital decay rate, by Finn and Sutton [26]

$$\frac{\dot{P}_{\rm b} - \dot{P}_{\rm b}^{\rm GR}}{\dot{P}_{\rm b}^{\rm GR}} = \frac{5}{24}\frac{\left(1-e^2\right)^3}{1+\frac{73}{24}e^2+\frac{37}{96}e^4}\left(\frac{P_{\rm b}}{2\pi\hbar}\right)^2 m_{\rm g}^2\,. \tag{12.16}$$

Here $\dot{P}_{\rm b}^{\rm GR}$ is the value predicted by the general relativity in Eq. (12.3). Notice that the fractional change is proportional to $\propto P_{\rm b}^2 m_{\rm g}^2$. Therefore, if the precision of $\dot{P}_{\rm b}$ is given, binary pulsars with larger orbits have a larger figure of merit for the test. However, usually, the precision of $\dot{P}_{\rm b}$ crucially depends on the orbital size, and it turns out that, still, binary pulsars with smaller orbits have a larger figure of merit.

The most recent constraint in this Finn-Sutton framework was provided by a combination of multiple best-timed binary pulsars with a Bayesian statistical treatment. A collection of nine best-timed binary pulsars (PSRs J0348+0432, J0737−3039, J1012+5307, B1534+12, J1713+0747, J1738+0333, J1909−3744, B1913+16, and J2222−0137) provide a tight bound on the graviton mass,

$$m_g < 5.2\times10^{-21}\,\mathrm{eV}/c^2, \quad (90\%\ \mathrm{C.L.})\,, \tag{12.17}$$

using a uniform prior in $\ln m_{\rm g}$ [44]. This limit is not the strongest limit on the graviton mass [22]. However, from a theoretical point of view, it is a bound from binary orbital dynamics, complementary to, e.g. the kinematic dispersion-relation

[6] The conditions are that (i) the wave equation takes a standard form for the trace-reversed metric perturbation $\bar{h}_{\mu\nu}$

$$\left(\Box - m_{\rm g}^2\right)\bar{h}_{\mu\nu} + 16\pi T_{\mu\nu} = 0\,, \tag{12.15}$$

and the theory recovers the general relativity in the limit when $m_{\rm g} \to 0$, namely, there is no van Dam-Veltman-Zakharov discontinuity [26].

tests from the LIGO/Virgo/KAGRA observation of gravitational waves [5]. It is worth mentioning that the theory (12.14) has some drawbacks including ghosts and instability [22, 26], and here it is only used as a strawman target for illustration.

? Exercise

12.6. Derive the lower limit for the Compton wavelength of gravitons from Eq. (12.17).

It is interesting to note, that in different massive gravity theories, the dependence of the extra radiation on the graviton mass is in general different. It depends on the specifics of the illustrated gravity theory. This is due to the deep fundamental principles in the designs of a number of variants of massive gravity theories. For example, in a cosmologically motivated massive gravity theory, known as the *cubic Galileon theory* with the action [21],

$$S = \int \mathrm{d}^4x \left[-\frac{1}{4} h^{\mu\nu} (\mathcal{E}h)_{\mu\nu} + \frac{h^{\mu\nu} T_{\mu\nu}}{2M_{\rm Pl}} - \frac{3}{4} (\partial\varphi)^2 \left(1 + \frac{1}{3m_{\rm g}^2 M_{\rm Pl}} \Box\varphi \right) + \frac{\varphi T}{2M_{\rm Pl}} \right], \tag{12.18}$$

the specific way of the addition of the scalar field φ introduces the so-called *screening mechanism*, thus avoids the stringent constraints from the Solar System, yet provides important changes to the cosmological evolution. In the action (12.18), φ is the Galileon scalar field, $T_{\mu\nu}$ is the matter energy-momentum tensor, $T \equiv T^{\mu}{}_{\mu}$, $M_{\rm Pl}$ is the Planck mass, and

$$(\mathcal{E}h)_{\mu\nu} \equiv -\frac{1}{2} \Box h_{\mu\nu} + \cdots \tag{12.19}$$

is the Lichnerowicz operator. For a central massive body with mass M, the *screening radius* is $r_\star = \left(M / 16 m_{\rm g}^2 M_{\rm Pl}^2 \right)^{1/3}$, within which, the theory exhibits strong couplings and it reduces to the canonical gravity.

? Exercise

12.7. By knowing that the Earth is within the screening radius of the Sun, derive the upper limit of graviton mass in the cubic Galileon theory.

According to de Rham et al. [21], though with a screening mechanism to suppress modification at the high density region within $r_\star$, this cubic Galileon theory predicts

a different scaling behaviour for the gravitational radiation. For a system with a typical length scale L, the *fifth-force* suppression factor is $\sim \left(L/r_\star\right)^{3/2}$, and the suppression factor for the gravitational radiation is $\sim (P_\mathrm{b}/r_\star)^{3/2}$. As for a binary system, one has $L \sim v P_\mathrm{b}$ where v is a characteristic velocity. Therefore, the gravitational radiation is, compared with the fifth force, *less* suppressed by a factor of $v^{3/2}$, and it provides a valuable window to look for evidence of this theory via radiative channels, for example, in binary pulsar systems.

Analytic radiative powers were worked out by de Rham et al. [21], and the extra radiative channels include monopolar radiation, dipolar radiation, and quadrupolar radiation. For binary pulsar systems with different orbital periods and orbital eccentricities, the dominate radiation channel can be different [55]. For the current set of binary pulsars, the quadrupole radiation is the dominating factor among the extra channels [21, 55].

The most up-to-date constraint from binary pulsars is

$$m_g < 2 \times 10^{-28}\,\mathrm{eV}/c^2, \quad (95\%\ \mathrm{C.L.})\,, \tag{12.20}$$

for the cubic Galileon theory, and the cumulative probability distributions of the graviton mass are given in Fig. 12.3 for two different priors [55]. Such a tight constraint was obtained from the combination of fourteen best-timed binary pulsar systems, including PSRs J0348+0432, J0437−4715, J0613−0200, J0737−3039, J1012+5307, J1022+1001, J1141−6545, B1534+12, J1713+0747, J1738+0333, J1756−2251, J1909−3744, B1913+16, and J2222−0137. One should keep in mind that, the limit (12.20) is theory specific, and in this situation, only applies to the cubic Galileon theory given in Eq. (12.18). Nonetheless, it provides an interesting example that for a gravity theory designed for cosmological purposes at corresponding lengthscales, binary pulsar systems with astronomical lengthscales still provide intriguing and useful bounds. It is an illustration of using binary pulsars

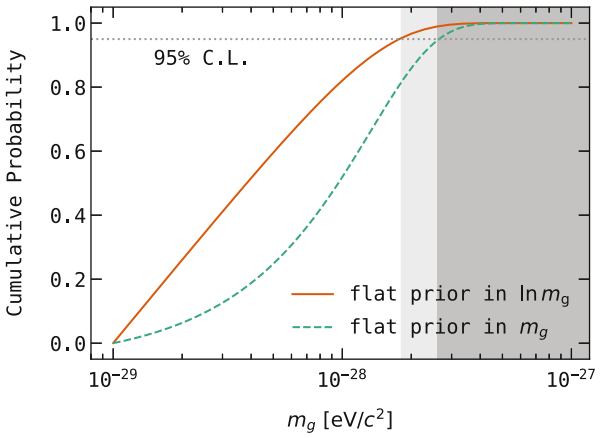

Fig. 12.3 Cumulative probability for the graviton mass with two different priors in the cubic Galileon theory [55]. Shaded regions show the excluded graviton mass values at the 95% confidence level

in the studies of cosmology by examining the modification to binary orbits brought by a cosmologically-motivated modified gravity.

12.4 Strong Equivalence Principle and Dark Matters

Binary pulsars are not only useful for the radiative tests introduced in the above sections, they also provide superb limiting power in the conservative aspects of gravitational dynamics for orbital evolutions. Below we introduce an example of examining the strong equivalence principle via the conservative dynamics of binary pulsars [18, 72], and its extension to test certain interesting properties of dark matters [54, 60].

As discovered by Damour and Schäfer [18], a perturbed binary orbit with an equivalence-principle-violating abnormal acceleration has a characteristic evolution in its orbital elements. The notable change is the appearance of a *vectorized superposition* of two eccentricity vectors for the real orbital eccentricity. It provides a graphical understanding of the underlying dynamics for a binary in presence of equivalence principle violations. The *real* orbital eccentricity vector, $\boldsymbol{e}(t)$, is an addition of a rotating normal eccentricity vector, $\boldsymbol{e}_{\rm R}(t)$, in its post-Newtonian fashion, and an extra abnormal eccentricity vector, $\boldsymbol{e}_\Delta$, which is time independent and whose length is proportional to the Eötvös parameter, Δ, describing the violation of the equivalence principle. If $\Delta = 0$, the abnormal eccentricity vector $\boldsymbol{e}_\Delta = 0$ and it returns to the precessing case in the general relavitity. A graphical illustration is given in Fig. 12.4. As we discussed in Sect. 12.1, the pulsar timing

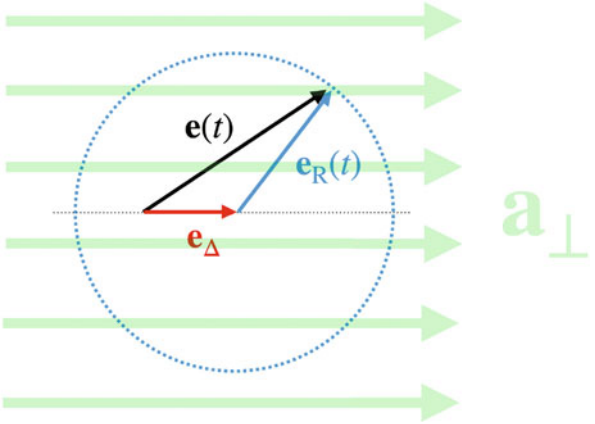

Fig. 12.4 Graphical illustration of the time-varying orbital eccentricity vector, $\boldsymbol{e}(t)$, for a binary pulsar, in the presence of strong equivalence principle violation [18]. The orbital eccentricity vector evolves according to $\boldsymbol{e}(t) = \boldsymbol{e}_\Delta + \boldsymbol{e}_{\rm R}(t)$, where $\boldsymbol{e}_{\rm R}(t)$ is the usual precessing eccentricity vector in the general relativity, and the *constant* abnormal eccentricity is in the direction of $\boldsymbol{a}_\perp$, which is the projection of the external Galactic acceleration in the orbital plane

technique is very sensitive to tiny changes in the orbit, and such a change can be captured in pulsar timing data [18].

At the beginning, such a scenario was applied to a few binary pulsars in a statistical sense by marginalizing over some unknown angles to obtain constraints on the violation of the equivalence principle [18]. Later it was implemented to a handful of binary pulsars with an improved statistical methodology to better account for the movements of binary pulsars in the Milky Way [63]. Then, with better data and more information about binary pulsar systems, a direct method was developed [27]. The direct method not only can constrain the equivalence principle violation, but in principle can detect it if it exists.

The most stringent limit using binary pulsars comes from a precisely timed long-orbital-period binary pulsar, PSR J1713+0747 [72], as larger orbits have higher figures of merit in such a test [18]. Using the improved direct method, the limit on the Eötvös parameter from PSR J1713+0747 is [72],

$$|\Delta| < 2 \times 10^{-3}\,, \quad (95\%\ \text{C.L.})\,. \tag{12.21}$$

Though it is much less limiting than the earlier constraint obtained from the Solar System [60, 65], the limit (12.21) encodes strong-field effects. For example, in the case of the aforementioned scalar-tensor gravity, the strong-field version of Eötvös parameter will be very different from its weak-field counterpart [27]. Therefore, such a limit from neutron stars is a *standalone* bound and applicable to the strong version of equivalence principle [51, 63].

The limit (12.21) is not only interesting to gravitational physics, it also has its value when we look at it from a different angle. As we now know, the binary pulsar is actually immersed in the ocean of dark matters in the Milky Way. As we have not really understood what the very nature of dark matter is, the above method for testing the equivalence principle provides a non-traditional probe to dark matter's properties. Shao et al. [54] proposed a method where such a limit, with a proper handle, can be converted to the interaction properties between dark matters and ordinary matters.

If there is a *long-range fifth force* between dark matter particles and ordinary matter fields, as many field theories will suggest [60], it is likely to introduce an *apparent* violation of the strong equivalence principle if we have not taken the fifth force into account in our standard assumptions. The role of the Galactic acceleration in Fig. 12.4, whose projection on the orbital plane is $\boldsymbol{a}_\perp$, is replaced by the attraction of dark matters to the binary system. The difference in the acceleration to two binary components (a neutron star and a white dwarf in the case of PSR J1713+0747), described by Δ, is replaced by a quantity related to the long-range fifth-force between dark matters and ordinary standard-model matters [54].

Detailed analysis of PSR J1713+0747 [54] took into consideration of the Galactic distribution of dark matters, and gave a very different bound in nature that could be obtained from terrestrial experiments [60]. The current observational data of PSR J1713+0747 already imply that, if there is such a long-range fifth force between dark matters and ordinary matters, its magnitude should be no more than 1% of

the gravitational force between them. Such a limit provides a useful complement to other types of dark-matter experiments, which are usually looking for *short-range* forces between the hypothesized dark-matter particles and the standard-model particles [60], including the searches in underground laboratories, particle colliders, and X-ray/γ-ray observations via high-energy satellites.

12.5 Summary

In this chapter, we present some basic concepts of using binary pulsars as *fundamental clocks* in a curved spacetime to probe various types of modifications to the binary orbits. These modifications could have been caused by a modified gravity theory or some other new physics like a long-range fifth force between dark matters and ordinary matters. As pulsar timing provides us with very *accurate* measurements, it puts constraints on tiny changes caused by an alternative gravity theory other than the general relativity. Moreover, neutron stars are intrinsically *strong-gravity* objects, and nonperturbative aspects of the strong-field gravity can also be studied via radio pulsar experiments. Actually, quite many strong-field limits are still best provided by pulsar timing experiments, even nowadays in presence of new types of observations like gravitational waves and black hole shadows. A careful study shows that the limits from pulsar timing are actually complementary to those from gravitational wave detections and black hole shadows [8, 53]. Proper combinations of these strong-gravity experiments could provide a more complete landscape to gravitation in the strong-field .

Solely focusing on the radio pulsar side, the timing experiments can be carried out for decades, in particular for some interesting systems like the Hulse-Taylor pulsar PSR B1913+16 [61] and the Double Pulsar PSR J0737−3039A/B [37]. Long-term observations improve the precision of PPK parameters with the observational time span $T_{\rm obs}$. For examples, the precision in the orbital decay parameter, $\dot{P}_{\rm b}$, improves very fast, as $T_{\rm obs}^{-5/2}$, and the precision in the periastron advance rate, $\dot{\omega}$, improves as $T_{\rm obs}^{-3/2}$. Furthermore, the sensitivity of radio telescopes is also improving, notably with the Five-hundred-meter Aperture Spherical Telescope in China [33, 40] and the Square Kilometre Array in South Africa and Australia [52, 62]. The former has already been operating for a couple of years, while the latter has also entered the construction phase recently. The improvement in the sensitivity of radio telescopes directly converts to improvements in the timing precision. Therefore, the real improvement for PPK parameters is faster than the theoretical power law predictions. Last but not the least, radio telescopes are also continuously discovering new pulsar systems, and some of these systems with suitable system properties will contribute to strong-field gravity tests. We are even looking forward to discovering yet-undetected binary pulsar systems like neutron-star black-hole binaries with short orbital periods $P_{\rm b} \lesssim 1$ day or pulsars around the Sgr A* black hole with orbital periods $P_{\rm b} \lesssim 10$ years [11, 12, 38], which will provide completely new gravity tests in the strong-field regimes [36].

Acknowledgments We are grateful to the 740th WE-Heraeus-Seminar "Experimental Tests and Signatures of Modified and Quantum Gravity", organized by Christian Pfeifer and Claus Lämmerzahl. LS was supported by the National SKA Program of China (2020SKA0120300), the National Natural Science Foundation of China (11975027, 11991053, 11721303), and the Max Planck Partner Group Program funded by the Max Planck Society.

References

1. B.P. Abbott et al., GW170817: observation of gravitational waves from a binary beutron star inspiral. Phys. Rev. Lett. **119**(16), 161101 (2017)
2. B.P. Abbott et al., Tests of General Relativity with GW170817. Phys. Rev. Lett. **123**(1), 011102 (2019)
3. B.P. Abbott et al., Tests of General Relativity with the Binary Black Hole Signals from the LIGO-Virgo Catalog GWTC-1. Phys. Rev. D **100**(10), 104036 (2019)
4. R. Abbott et al., Tests of general relativity with binary black holes from the second LIGO-Virgo gravitational-wave transient catalog. Phys. Rev. D **103**(12), 122002 (2021)
5. R. Abbott et al., Tests of general relativity with GWTC-3 (2021). arXiv:2112.06861
6. K. Akiyama et al., First M87 event horizon telescope results. I. the shadow of the supermassive black hole. Astrophys. J. Lett. **875**L1 (2019)
7. K. Akiyama et al., First sagittarius A* event horizon telescope results. I. the shadow of the supermassive black hole in the center of the milky way. Astrophys. J. Lett. **930**(2), L12 (2022)
8. K. Akiyama et al., First sagittarius A* event horizon telescope results. VI. testing the black hole metric. Astrophys. J. Lett. **930**(2), L17 (2022)
9. A.M. Archibald, N.V. Gusinskaia, J.W.T. Hessels, A.T. Deller, D.L. Kaplan, D.R. Lorimer, R.S. Lynch, S.M. Ransom, I.H. Stairs, Universality of free fall from the orbital motion of a pulsar in a stellar triple system. Nature **559**(7712), 73–76 (2018)
10. E. Berti, et al., Testing general relativity with present and future astrophysical observations. Class. Quant. Grav. **32**, 243001 (2015)
11. G.C. Bower, et al., Galactic Center Pulsars with the ngVLA. ASP Conf. Ser. **517**, 793 (2018)
12. G.C. Bower, et al., Fundamental Physics with Galactic Center Pulsars. Bull. Am. Astron. Soc. **51**(3), 438 (2019)
13. C. Brans, R.H. Dicke, Mach's principle and a relativistic theory of gravitation. Phys. Rev. **124**, 925–935 (1961)
14. M. Burgay, et al., An increased estimate of the merger rate of double neutron stars from observations of a highly relativistic system. Nature **426**, 531–533 (2003)
15. T. Damour, N. Deruelle, General relativistic celestial mechanics of binary systems. II. The post-Newtonian timing formula. Ann. Inst. Henri Poincaré Phys. Théor. **44**, 263–292 (1986)
16. T. Damour, G. Esposito-Farèse, Nonperturbative strong field effects in tensor-scalar theories of gravitation. Phys. Rev. Lett. **70**, 2220–2223 (1993)
17. T. Damour, G. Esposito-Farèse, Tensor-scalar gravity and binary pulsar experiments. Phys. Rev. D **54**, 1474–1491 (1996)
18. T. Damour, G. Schaefer, New tests of the strong equivalence principle using binary pulsar data. Phys. Rev. Lett. **66**, 2549–2552 (1991)
19. T. Damour, J.H. Taylor, Strong field tests of relativistic gravity and binary pulsars. Phys. Rev. D **45**, 1840–1868 (1992)
20. V.I. Danchev, D.D. Doneva, S.S. Yazadjiev, Constraining scalarization in scalar-Gauss-Bonnet gravity through binary pulsars. Phys. Rev. D **106**, 124001 (2022)
21. C. de Rham, A.J. Tolley, D.H. Wesley, Vainshtein mechanism in binary pulsars. Phys. Rev. D **87**(4), 044025 (2013)
22. C. de Rham, J.T. Deskins, A.J. Tolley, S.-Y. Zhou, Graviton mass bounds. Rev. Mod. Phys. **89**(2), 025004 (2017)

23. D.D. Doneva, S.S. Yazadjiev, New Gauss-Bonnet black holes with curvature-induced scalarization in extended scalar-tensor theories. Phys. Rev. Lett. **120**(13), 131103 (2018)
24. D.M. Eardley, Observable effects of a scalar gravitational field in a binary pulsar. Astrophys. J. **196**, L59–L62 (1975)
25. G. Esposito-Farèse, Tests of scalar-tensor gravity. AIP Conf. Proc. **736**(1), 35–52 (2004)
26. L.S. Finn, P.J. Sutton, Bounding the mass of the graviton using binary pulsar observations. Phys. Rev. D **65**, 044022 (2002)
27. P.C.C. Freire, M. Kramer, N. Wex, Tests of the universality of free fall for strongly self-gravitating bodies with radio pulsars. Class. Quant. Grav. **29**, 184007 (2012)
28. P.C.C. Freire, N. Wex, G. Esposito-Farèse, J.P.W. Verbiest, M. Bailes, B.A. Jacoby, M. Kramer, I.H. Stairs, J. Antoniadis, G.H. Janssen, The relativistic pulsar-white dwarf binary PSR J1738+0333 II. The most stringent test of scalar-tensor gravity. Mon. Not. R. Astron. Soc. **423**, 3328 (2012)
29. M. Guo, J. Zhao, L. Shao, Extended reduced-order surrogate models for scalar-tensor gravity in the strong field and applications to binary pulsars and gravitational waves. Phys. Rev. D **104**(10), 104065 (2021)
30. G. Hobbs, et al., Development of a pulsar-based timescale. Mon. Not. R. Astron. Soc. **427**, 2780–2787 (2012)
31. H. Hu, M. Kramer, N. Wex, D.J. Champion, M.S. Kehl, Constraining the dense matter equation-of-state with radio pulsars. Mon. Not. R. Astron. Soc. **497**(3), 3118–3130 (2020)
32. Z. Hu, Y. Gao, R. Xu, L. Shao, Scalarized neutron stars in massive scalar-tensor gravity: X-ray pulsars and tidal deformability. Phys. Rev. D **104**(10), 104014 (2021)
33. P. Jiang, et al., Commissioning progress of the FAST. Sci. China Phys. Mech. Astron. **62**(5), 959502 (2019)
34. M. Khalil, R.F.P. Mendes, N. Ortiz, J. Steinhoff, Effective-action model for dynamical scalarization beyond the adiabatic approximation. Phys. Rev. D **106**, 104016 (2022)
35. M. Kramer, Pulsars as probes of gravity and fundamental physics. Int. J. Mod. Phys. D **25**(14), 1630029 (2016)
36. M. Kramer, D.C. Backer, J.M. Cordes, T.J.W. Lazio, B.W. Stappers, S. Johnston, Strong-field tests of gravity using pulsars and black holes. New Astron. Rev. **48**, 993–1002 (2004)
37. M. Kramer, et al., Strong-field gravity tests with the double pulsar. Phys. Rev. X **11**(4), 041050 (2021)
38. K. Liu, R.P. Eatough, N. Wex, M. Kramer, Pulsar–black hole binaries: prospects for new gravity tests with future radio telescopes. Mon. Not. R. Astron. Soc. **445**(3), 3115–3132 (2014)
39. D.R. Lorimer, M. Kramer, Handbook of Pulsar Astronomy. Cambridge University Press, Cambridge (2005)
40. J. Lu, K. Lee, R. Xu, Advancing Pulsar Science with the FAST. Sci. China Phys. Mech. Astron. **63**(2), 229531 (2020)
41. A.G. Lyne, et al., A double-pulsar system: a rare laboratory for relativistic gravity and plasma physics. Science **303**, 1153–1157 (2004)
42. R.N. Manchester, Pulsars and gravity. Int. J. Mod. Phys. D **24**(06), 1530018 (2015)
43. R.N. Manchester, G.B. Hobbs, A. Teoh, M. Hobbs, The Australia Telescope National Facility pulsar catalogue. Astron. J. **129**, 1993 (2005)
44. X. Miao, L. Shao, B.-Q. Ma, Bounding the mass of graviton in a dynamic regime with binary pulsars. Phys. Rev. D **99**(12), 123015 (2019)
45. F.M. Ramazanoğlu, F. Pretorius, Spontaneous scalarization with massive fields. Phys. Rev. D **93**(6), 064005 (2016)
46. N. Sennett, L. Shao, J. Steinhoff, Effective action model of dynamically scalarizing binary neutron stars. Phys. Rev. D **96**(8), 084019 (2017)
47. L. Shao, Testing the strong equivalence principle with the triple pulsar PSR J0337+1715. Phys. Rev. D **93**(8), 084023 (2016)
48. L. Shao, Degeneracy in Studying the Supranuclear Equation of State and Modified Gravity with Neutron Stars. AIP Conf. Proc. **2127**(1), 020016 (2019)
49. L. Shao, General relativity withstands double pulsar's scrutiny. APS Phys. **14**, 173 (2021)

50. L. Shao, Imaging supermassive black hole shadows with a global very long baseline interferometry array. Front. Phys. (Beijing) **17**(4), 44601 (2022)
51. L. Shao, N. Wex, Tests of gravitational symmetries with radio pulsars. Sci. China Phys. Mech. Astron. **59**(9), 699501 (2016)
52. L. Shao, et al., Testing gravity with pulsars in the SKA era, in *Advancing Astrophysics with the Square Kilometre Array*, vol. AASKA14. Proceedings of Science (2015), p. 042
53. L. Shao, N. Sennett, A. Buonanno, M. Kramer, N. Wex, Constraining nonperturbative strong-field effects in scalar-tensor gravity by combining pulsar timing and laser-interferometer gravitational-wave detectors. Phys. Rev. X **7**(4), 041025 (2017)
54. L. Shao, N. Wex, M. Kramer, Testing the universality of free fall towards dark matter with radio pulsars. Phys. Rev. Lett. **120**(24), 241104 (2018)
55. L. Shao, N. Wex, S.-Y. Zhou, New graviton mass bound from binary pulsars. Phys. Rev. D **102**(2), 024069 (2020)
56. H.O. Silva, J. Sakstein, L. Gualtieri, T.P. Sotiriou, E. Berti, Spontaneous scalarization of black holes and compact stars from a Gauss-Bonnet coupling. Phys. Rev. Lett. **120**(13), 131104 (2018)
57. I.H. Stairs, Testing general relativity with pulsar timing. Living Rev. Rel. **6**, 5 (2003)
58. J.H. Taylor, Pulsar timing and relativistic gravity. Phil. Trans. A. Math. Phys. Eng. Sci. **341**(1660), 117–134 (1992)
59. G. Voisin, I. Cognard, P.C.C. Freire, N. Wex, L. Guillemot, G. Desvignes, M. Kramer, G. Theureau, An improved test of the strong equivalence principle with the pulsar in a triple star system. Astron. Astrophys. **638**, A24 (2020)
60. T.A. Wagner, S. Schlamminger, J.H. Gundlach, E.G. Adelberger, Torsion-balance tests of the weak equivalence principle. Class. Quant. Grav. **29**, 184002 (2012)
61. J.M. Weisberg, Y. Huang, Relativistic measurements from timing the binary pulsar PSR B1913+16. Astrophys. J. **829**(1), 55 (2016)
62. A. Weltman, et al., Fundamental Physics with the Square Kilometre Array. Publ. Astron. Soc. Austral. **37**, e002 (2020)
63. N. Wex, Testing relativistic gravity with radio pulsars, in *Frontiers in Relativistic Celestial Mechanics: Applications and Experiments*, ed. by S.M. Kopeikin, vol. 2 (Walter de Gruyter GmbH, Berlin/Boston, 2014), p. 39
64. N. Wex, M. Kramer, Gravity tests with radio pulsars. Universe **6**(9), 156 (2020)
65. C.M. Will. The confrontation between general relativity and experiment. Living Rev. Rel. **17**, 4 (2014)
66. R. Xu, Y. Gao, L. Shao, Strong-field effects in massive scalar-tensor gravity for slowly spinning neutron stars and application to X-ray pulsar pulse profiles. Phys. Rev. D **102**(6), 064057 (2020)
67. R. Xu, Y. Gao, L. Shao, Neutron stars in massive scalar-Gauss-Bonnet gravity: Spherical structure and time-independent perturbations. Phys. Rev. D **105**(2), 024003 (2022)
68. K. Yagi, D. Blas, E. Barausse, N. Yunes, Constraints on Einstein-Æther theory and Hořava gravity from binary pulsar observations. Phys. Rev. D **89**(8), 084067 (2014). Erratum: Phys.Rev.D 90, 069902 (2014), Erratum: Phys.Rev.D 90, 069901 (2014)
69. S.S. Yazadjiev, D.D. Doneva, D. Popchev, Slowly rotating neutron stars in scalar-tensor theories with a massive scalar field. Phys. Rev. D **93**(8), 084038 (2016)
70. J. Zhao, L. Shao, Z. Cao, B.-Q. Ma, Reduced-order surrogate models for scalar-tensor gravity in the strong field regime and applications to binary pulsars and GW170817. Phys. Rev. D **100**(6), 064034 (2019)
71. J. Zhao, P.C.C. Freire, M. Kramer, L. Shao, N. Wex, Closing a spontaneous-scalarization window with binary pulsars. Class. Quant. Grav. **39**(11), 11LT01 (2022)
72. W.W. Zhu, et al., Tests of gravitational symmetries with pulsar binary J1713+0747. Mon. Not. R. Astron. Soc. **482**(3), 3249–3260 (2019)